Study of μm-scale spatial variations in strain of a compositionally step-graded In$_x$Ga$_{1-x}$As/GaAs(001) heterostructure

K. Rammohan and D. H. Rich[a]
Photonic Materials and Devices Laboratory, Department of Materials Science and Engineering, University of Southern California, Los Angeles, California 90089-0241

R. S. Goldman, J. Chen, H. H. Wieder, and K. L. Kavanagh
Department of Electrical and Computer Engineering, University of California at San Diego, La Jolla, California 92093-0407

The relaxation of strain in compositionally step-graded In$_x$Ga$_{1-x}$As layers grown on GaAs(001) has been examined with cathodoluminescence (CL) wavelength and linearly polarized imaging approaches. A polarization anisotropy in CL is found, and this correlates with spectral shifts in the peak positions of excitonic luminescence. Varying asymmetries in misfit dislocation densities from transmission electron microscopy are found to be consistent with the μm-scale spatial variations in strain that is deduced from the CL. © *1995 American Institute of Physics.*

The interest in lattice-mismatched III–V semiconductor materials is driven, not only by the possibility of creating optoelectronic devices such as light modulators, lasers, and detectors with tunable energy sensitivity, but also by the possibility of integrating existing III–V devices with current Si technology. The approach is to create a defect-filtering buffer layer that is grown between the surface device structure and the substrate. Recent experiments with relatively thin (less than ~ 1 μm thick) compositionally step- and linearly graded buffer layers have been successful in producing close to 100% relaxed layers with threading dislocation densities less than $\sim 10^6$ cm^{-2}. Such results have been reported for a variety of lattice-mismatched systems including Ge/Si,[1,2] In$_{0.5}$Ga$_{0.5}$As/GaAs,[3–5] and In$_{0.4}$Ga$_{0.6}$P/GaP.[6] However, with incomplete strain relaxation, such systems can exhibit an anisotropic in-plane strain relaxation as measured by multiple-crystal x-ray diffraction[5] and deduced from the nonuniform and anisotropic misfit dislocation densities that have been observed in plan-view transmission electron microscopy (TEM) studies.[7]

In this letter, we have performed an examination of spatial variations in strain and alloy composition of a step-graded In$_x$Ga$_{1-x}$As/GaAs buffer layer heterostructure using two new variations in the cathodoluminescence (CL) imaging technique. A unique combination of scanning linearly polarized CL (LPCL)[8] and CL wavelength imaging (CLWI)[9] measurements were performed. In CLWI, the wavelength [$\lambda_m(x,y)$], at which there is a peak in the intensity of a luminescence spectrum, is determined as a function of the spatial (x,y) position, and a false-color or greyscale image directly mapping these wavelengths is generated.[9] A North Coast EO-817 Ge p-i-n detector was used to measure the signal dispersed by a 0.25 m monochromator. An electron beam energy of 20 keV and a beam current of 10 nA were used to probe the sample, maintained at 87 K, for the CL measurements.

The sample studied was grown by solid source molecular beam epitaxy on a GaAs(001) wafer offcut 2° toward (011). The structure consists of a four step-graded In$_x$Ga$_{1-x}$As buffer layer, each step doped n-type (10^{18} cm^{-3}) and grown 2000 Å thick with nominal In mole fractions of $x = 0.05$, 0.10, 0.15, and 0.20, respectively. Plan-view TEM was used to determine misfit dislocation densities.

A CLWI micrograph of the step-graded structure is shown in Fig. 1(a). The mapping of λ_m into the greyscale representation is shown by the grey bar indicating the wave-
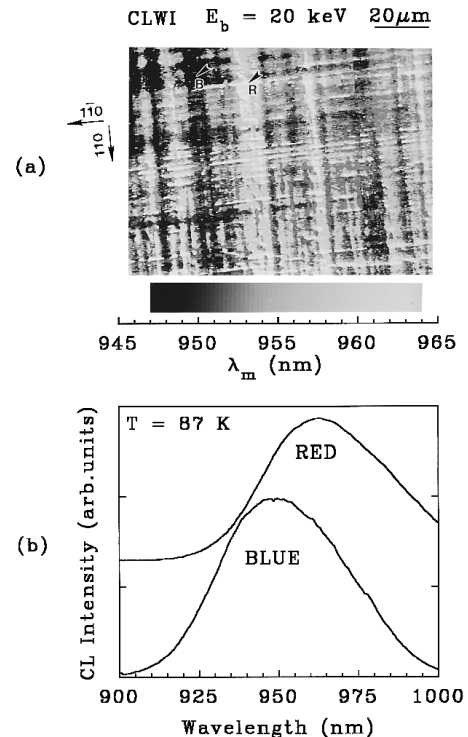
FIG. 1. CL wavelength imaging in (a) and local CL spectra in (b) for two different positions. A scale showing the mapping of wavelengths of peak CL intensity into shades of grey is shown in (a). The blue- and red-shifted local spectra in (b) were obtained from the spatial positions labeled B and R, respectively, with arrows in (a).

[a]Author to whom correspondence should be addressed.
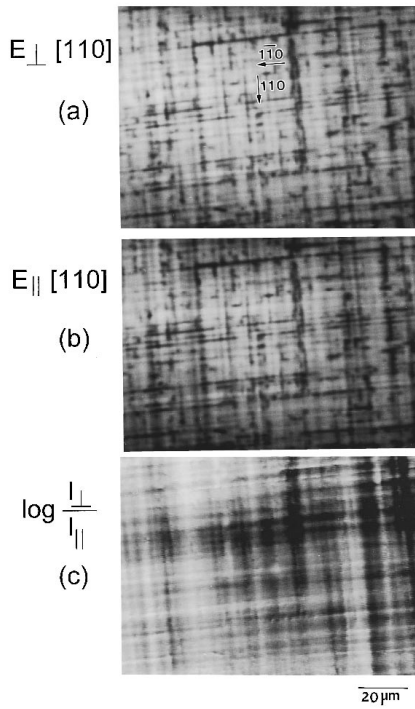
FIG. 2. Monochromatic linearly polarized CL images for same region shown in Fig. 1(a) at $\lambda = 956$ nm. The polarization detection conditions of $\mathbf{E} \perp [110]$ and $\mathbf{E} \| [110]$ are shown in (a) and (b), respectively. The ratio image of $\log(I_\perp / I_\|)$ is shown in (c), revealing the μm-scale polarization anisotropy.

FIG. 3. Plan-view TEM showing two different regions of the $In_{0.15}Ga_{0.85}As/In_{0.20}Ga_{0.80}As$ interface which exhibits different dislocation densities and strain relaxation along both $\langle 110 \rangle$ directions in (a) and (b).

length scale. Local CL spectra are shown in Fig. 1(b); these spectra were obtained while fixing the electron beam at typical blue- and red-shifted positions, as indicated by the grey-scale representation for λ_m in the image of Fig. 1(a). A shift of ~14 nm (~19 meV) is seen between these blue- and red-shifted regions. The full-width at half-maximum of both spectra is ~47 nm (~64 meV), and this large width results from CL contributions stemming from the different layers in the buffer region, each of which has a different contribution to the overall spectra. The excitonic transitions occurring in each of the four $In_xGa_{1-x}As$ buffer layers are not resolved as a result of inhomogeneous broadening caused by local sub-μm random strain variations, a large density of defects in the underlying $In_xGa_{1-x}As$ layers, and fluctuations in alloy composition.

Long streaks of constant grey shade are found to run along the high symmetry $\langle 110 \rangle$ directions in Fig. 1(a). These streaks correlate with the orientation and position of dark line defects (DLDs) of this sample, as observed in the LPCL images of Figs. 2(a) and 2(b). DLDs are typically observed in the monochromatic CL imaging of partially relaxed InGaAs films grown on GaAs.[10] The LPCL images of Figs. 2(a) and 2(b) were taken with the polarizer rotated to detect emission of light with $\mathbf{E} \perp [110]$ and $\mathbf{E} \| [110]$ detection orientations at a wavelength of 956 nm (1296 meV), where $\mathbf{E}$ is the electric field of the light. In order to emphasize polarization variations in luminescence, the ratio of these images is displayed in Fig. 2(c). The pixels in the ratio image at a (x,y) position are represented as $\log[I_\perp(x,y)/I_\|(x,y)]$, where $I_\perp$ and $I_\|$ are the pixel intensities under $\mathbf{E} \perp [110]$ and $\mathbf{E} \| [110]$ detection orientations, normalized to a 256 level greyscale.
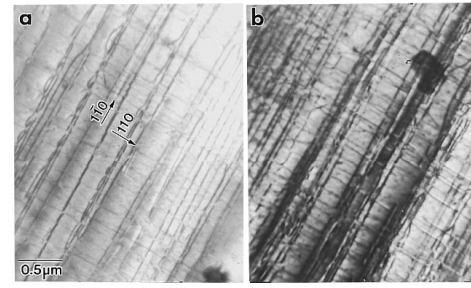
The bright and dark regions in Fig. 2(c) correspond to intensity ratios, $I_\perp / I_\|$, of ~0.9 and ~0.6, respectively. The average value of $I_\perp / I_\|$ is 0.83, as measured from integrated LPCL spectra taken while the electron beam is rapidly scanning the entire region shown in Fig. 2(c). It is our hypothesis that the presence of bright and dark streaks (i.e., a nonuniform intensity) in Fig. 2(c), running parallel to the DLDs in Figs. 2(a) and 2(b), reveals a polarization anisotropy caused by μm-scale variations in strain.

The strain-induced splitting of the heavy-hole (hh) and light-hole (lh) valence bands at $\mathbf{k}=0$ can be studied by examining the polarization and energy dependence of the luminescence.[8,11] The energy change, ΔE, of the excitonic luminescence involving the $j=3/2$ valence bands induced by the strain is given by the following solution of the orbital-strain Hamiltonian for $\mathbf{k}=0$:[11]

$$\Delta E = -a(\epsilon_{xx} + \epsilon_{yy} + \epsilon_{zz})$$
$$\pm \frac{1}{2}\sqrt{4d^2\epsilon_{xy}^2 + b^2(2\epsilon_{zz} - \epsilon_{xx} - \epsilon_{yy})^2 + 3b^2(\epsilon_{xx} - \epsilon_{yy})^2},$$

(1)

where $\epsilon_{xx} = \epsilon_{yy} = (\epsilon_{110} + \epsilon_{1\bar{1}0})/2$, $\epsilon_{xy} = (\epsilon_{1\bar{1}0} - \epsilon_{110})/2$, and $\epsilon_{zz} = -2\epsilon_{xx}C_{12}/C_{11}$; ϵ_{110} and $\epsilon_{1\bar{1}0}$ are the strains along $[110]$ and $[1\bar{1}0]$ directions, respectively. The constant a is the hydrostatic deformation potential; b and d are uniaxial deformation potentials associated with strains of tetragonal and rhombohedral symmetries, respectively, which remove the degeneracy of the bands as indicated by the $\pm$ sign; C_{11} and C_{12} are elastic constants; these constants for $In_xGa_{1-x}As$ are found by interpolating between values for GaAs and InAs.[12]

We have examined the $In_{0.15}Ge_{0.85}As/In_{0.20}Ga_{0.80}As$ interface with plan-view TEM, as shown in Fig. 3. The misfit dislocation distribution, most of which are of the 60° type,[5,7] was examined at several different regions of the interface. Figures 3(a) and 3(b) show linear misfit dislocation densities of 6.1×10^4 and 8.0×10^4 cm^{-1} along $[1\bar{1}0]$ and 6.5×10^4 and 1.3×10^5 cm^{-1} along $[110]$, respectively. For 60° misfit dislocations, an average strain relaxation of 0.02% occurs for linear dislocation density of 1×10^4 cm^{-1}.[7] The resulting in-plane strains, ϵ_{110} and $\epsilon_{1\bar{1}0}$, in the $In_{0.20}Ga_{0.80}As$ film relative to a relaxed $In_{0.15}Ga_{0.85}As$ film are, respectively, 0.219% and 0.227% in Fig. 3(a) and 0.189% and 0.091% in Fig. 3(b). Application of Eq. (1) gives a ΔE of 19.3 ± 7.4 and 12.1 ± 5.1 meV for the regions of
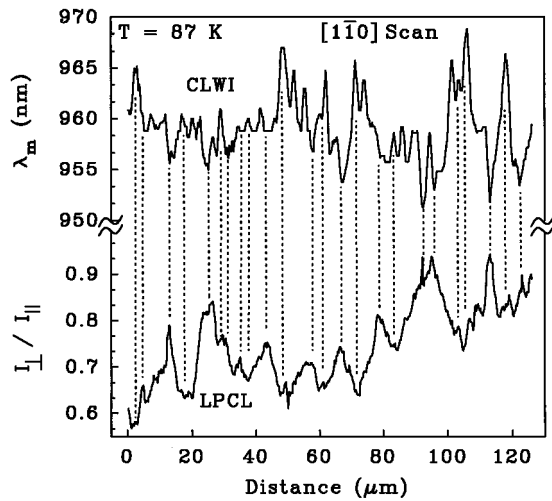
FIG. 4. Histogram of the CL wavelength imaging, CLWI, and $I_\perp/I_\parallel$ ratio for a line scan along [1$\bar{1}$0]. The spatial correlation of regions with a red shift and an increased polarization anisotropy (regions of nearly uniaxial compressive stress) and regions with a blue shift and a reduced polarization anisotropy (regions of nearly biaxial compressive stress) is observed.

Figs. 3(a) and 3(b), respectively; the center of the strain-split bands is separated by ~7 meV. It is, therefore, evident that regions of isotropic and anisotropic relaxation are both found in this sample. The regions of Figs. 3(a) and 3(b) represent typical variations sampled with TEM. The CL images represent a sampling over a much larger area, thereby enabling measurements of variations in transition energy [as, e.g., the ~19 meV shift seen in the CL spectra of Fig. 1(b)] which are greater than those estimated from the TEM analysis and Eq. (1).

For an in-plane biaxial stress (resulting in $\epsilon_{xy}=0$), no polarization of either hh- or lh-excitonic emissions is expected for emission normal to the (001) surface plane. For a pure uniaxial stress along the [110] direction, mixing of hh and lh characters in the strain-split bands is negligible, and hh (lh) excitonic emission normal to the (001) surface plane is totally (partially) linearly polarized perpendicular (parallel) to [110].[11] Since the interface exhibits varying degrees of relaxation along both ⟨110⟩ directions, there will be varying degrees of mixing of hh and lh characters in the strain split bands, leading to only a partial linear polarization for excitation emission. The regions of uniform bright and dark contrast in Fig. 2(c) indicate variations from nearly biaxial to uniaxial compressive stress, respectively, as the system relaxes preferentially along the [110] direction. Such anisotropic relaxation would create regions of quasiuniaxial stress which are observed to run along both ⟨110⟩ directions in Fig.

2(c). The bright streaks in Fig. 2(c) indicate regions where the intensity ratio $I_\perp/I_\parallel$, is closest to unity, revealing regions closest to biaxial stress. The dark streaks, likewise, run along both ⟨110⟩ directions, yield minima of $I_\perp/I_\parallel$, and reveal regions closest to a uniaxial stress.

A further correlation of the CLWI image of Fig. 1(a) with the LPCL image of Fig. 2(c) is shown with a peak wavelength and $I_\perp/I_\parallel$ ratio versus distance histogram in Fig. 4, taken along an arbitrary [1$\bar{1}$0]-oriented line. The histogram shows that the blue- and red-shifted regions in CLWI correspond to the regions of reduced- and enhanced-polarization anisotropy [bright and dark regions in Fig. 2(c)], respectively, in the LPCL imaging. This correlation confirms that the spatial variation in emission wavelengths, as shown in Fig. 1(a), is caused primarily by variations in in-plane strain as opposed to composition which would not yield a polarization anisotropy. The regions of anisotropic relaxation (quasiuniaxial) correspond to regions of primarily enhanced relaxation along [110]. These regions also correspond to a reduced total compressive stress along [110] which results in a red-shifted luminescence that is spatially correlated with a polarization anisotropy, as observed in Fig. 4.

In conclusion, we have studied the strain relaxation of compositionally step-graded $In_xGa_{1-x}As$ layers using LPCL, CLWI, and TEM. We have observed local μm-scale variations in compressive stress ranging from nearly uniaxial to biaxial, resulting in a marked polarization anisotropy concomitant with a variation in luminescence transition energy.

[1] E. A. Fitzgerald, Y.-H Xie, M. L. Green, D. Brasen, A. R. Kortan, J. Michel, Y.-J. Mii, and B. E. Weir, Appl. Phys. Lett. **59**, 811 (1991).

[2] F. K. LeGoues, B. S. Meyerson, and J. F. Morar, Phys. Rev. Lett. **66**, 2903 (1991).

[3] K. Chang, P. Bhattacharya, and R. Lai, J. Appl. Phys. **67**, 3323 (1990).

[4] K. Inoue, J. C. Harmand, and T. Matsuno, J. Cryst. Growth **111**, 313 (1991).

[5] J. C. P. Chang, J. Chen, J. M. Fernandez, H. H. Weider, and K. L. Kavanagh, Appl. Phys. Lett. **60**, 1129 (1992).

[6] T. P. Chin, J. C. P. Chang, K. L. Kavanagh, C. W. Tu, P. D. Kirchner, and J. M. Woodall, Appl. Phys. Lett. **62**, 2369 (1993).

[7] K. L. Kavanagh, M. A. Capano, L. W. Hobbs, J. C. Barbour, P. M. J. Maree, W. Schaff, J. W. Mayer, D. Pettit, J. M. Woodall, J. A. Stroscio, and R. M. Feenstra, J. Appl. Phys. **64**, 4843 (1988).

[8] D. H. Rich, A. Ksendzov, R. W. Terhune, F. J. Grunthaner, B. A. Wilson , H. Shen, M. Dutta, S. M. Vernon, and T. M. Dixon, Phys. Rev. B **43**, 6836 (1991).

[9] M. Grundmann, J. Christen, D. Bimberg, A. Hashiomoto, T. Fukunaga, and N. Watanabe, Appl. Phys. Lett. **58**, 2090 (1991).

[10] D. H. Rich, T. George, W. T. Pike, J. Maserjian, F. J. Grunthaner, and A. Larsson, J. Appl. Phys. **72**, 5834 (1992).

[11] F. H. Pollak and M. Cardona, Phys. Rev. **172**, 816 (1968).

[12] S. Adachi, J. Appl. Phys. **53**, 8775 (1982).